

State-of-the Art of Geotechnical Monitoring with Geodetic Techniques

W. Lienhart

Institute of Engineering Geodesy and Measurement Systems, Graz University of Technology, Graz, Austria

E-mail: werner.lienhart@tugraz.at

ABSTRACT: Within the last decades geodetic deformation monitoring has evolved from manual measurements of a small number of marked points to fully automated, large scale and high precision automatic warning systems. This article reviews the state-of-the art and discusses the potential of current geodetic techniques. It is demonstrated that modern geodetic techniques are capable to perform long-term measurements with millimetre or even sub millimetre accuracy over long distances and completely remotely. This is crucial especially in geotechnical monitoring where the structure may not be accessible due to safety reasons. The applicability of methods like laser scanning, robotic total stations, image based measurements and further more is demonstrated with case studies including the monitoring of landslides, retaining walls, pipelines and water dams.

KEYWORDS: Geotechnical monitoring, Total stations, Laser scanning, InSAR, GNSS, Photogrammetric measurements

1. INTRODUCTION

Geotechnical monitoring is used to assess the safety of manmade structures like tunnels, dams, piles, retaining walls or pipelines and to determine the behaviour of natural objects like rock faces, slopes or caves. To fulfil these tasks different geotechnical and geodetic measurement techniques are used.

Within the last decades, geodetic monitoring has evolved from manual measurements of a small number of marked points to fully automated, large scale and high precision automatic warning systems. This article reviews the state-of-the art and discusses the potential and limitations of current geodetic techniques. Special emphasis is placed on robotic total stations (RTS), terrestrial laser scanning (TLS) and image based measurements. Ground and space based interferometric synthetic aperture radar (InSAR) as well as Global Navigation Satellite Systems (GNSS) are also discussed. The applicability of these methods is demonstrated by case studies including the monitoring of landslides, retaining walls, pipelines and water dams.

2. GEODETIC TECHNIQUES

2.1 Overview

Geodetic instruments (Figure 1) usually perform measurements with respect to external, stable reference points. Therefore, not only distortions but also rigid body movements can be derived. As a consequence geodetic monitoring is well suited to detect long term structural deformations like settlements.



Figure 1 Examples of geodetic instruments: GNSS antenna (top left), laser scanner (top right), total station (bottom left), Ground based interferometric synthetic aperture radar (bottom right)

Furthermore, geodetic measurements enable remote monitoring. The instrument is usually not placed on the object itself but performs measurements from distances of up to several kilometres. With some techniques, i.e. total station measurements, access to the monitoring object is still required to mount targets on the object of interest. However, other techniques like laser scanning or image based measurements do not need physical contact of the object at any time. This saves time, costs and enhances safety. In some applications, e.g. a rock face with rock falls, human life would at risk if a person has to mount targets on the monitoring object.

Common to all geodetic instruments are measurements through the atmosphere. The current state of the atmosphere therefore influences the quality of the measurements. Geodetic refraction can increase measurement noise and may introduce biases (Lienhart, 2017). For instance, the travel time of an emitted laser beam depends on the current temperature, pressure and humidity along the measurement path. An in-depth understanding of the atmospheric impact on the measurements is therefore crucial to achieve the nominal accuracy of geodetic measurement techniques.

2.2 Recent Developments

Within the last decade, the degree of automation of geodetic sensors increased significantly. Today's robotic total stations are able to automatically find and track targets. Unmanned aerial vehicles (UAVs) follow autonomously predefined measurement paths and the analysis of 3D point clouds can be fully automated under certain conditions.

The data rate increased considerably and measurement rates of million points per second are already standard for some instrument types. Additionally, the measurement resolution improved which opens new application areas.

Finally, a paradigm shift from monitoring of single marked points of a structure to the monitoring of the whole structure can be seen. All of these aspects are discussed in more detail for individual instrument types in the following section.

3. TOTAL STATION MEASUREMENTS

3.1 Principle of robotic total station measurements

Total stations measure slope distances and horizontal and vertical angles from the setup point to reflective targets. The 3D coordinates of the target points can be derived from these measurements. The aiming to the targets can be performed manually or fully automatically. Total stations can be set up on portable tripods or placed on fixed structures like surveying pillars. The instrument can be set up on a point with known coordinates or the coordinates of the instrument can be determined by measurements to reference points with known coordinates. Crucial for monitoring is the stability of the

setup point which can be verified by various means (Lienhart, 2017). Deformations of object points can be determined with total stations with accuracies of 1 mm or better (Table 1). Crucial to achieve such an accuracy are the meteorological correction of the electro-optic distance measurement (EDM) (Rüeger, 1996) and the avoidance of beam bending which occurs if temperature gradients orthogonal to the line of sight are present. Distance measurements can be meteorologically corrected by measuring the air temperature, pressure and humidity or by applying the local scale parameter method (Brunner & Rüeger, 1992).

Modern instruments are able to continuously track targets and measure their 3D position with frequencies of up to 20 Hz (Lienhart et al., 2017). With such measurement rates dynamic measurements of engineering structures like foot bridges become possible (Lienhart & Ehrhart, 2015).

Table 1 Specifications of selected total stations for monitoring; (Trimble, 2017; Leica Geosystems AG, 2014a; Topcon, 2016)

Total Station	Angle Accuracy ¹	Distance Accuracy	Distance Range
Trimble S9 HP	0.5"	0.8mm + 1ppm	3.0km
Leica TM50	0.5"	0.6mm + 1ppm	3.5km
Topcon MS AXII	0.5"	0.8mm + 1ppm	3.5km

¹An angle accuracy of 0.5" corresponds to a deviation of 1.5 mm at a distance of 600m

3.2 Inner city monitoring using total stations

Today, total stations are commonly used for monitoring of buildings during large construction activities in cities. This is for instance the case if tunnels for underground lines are being built in densely populated areas. Examples of recent large monitoring installations are the North-South Line in Amsterdam with more than 70 permanent operating total stations (Michel et al, 2003) and the Durchmesserlinie in Zurich with about 80 total stations (Meyer and Eisenegger, 2011). The by far largest number of permanent running total stations is currently used in the Cross Rail project in London. In total more than 500 instruments monitor continuously the impact of underground constructions on buildings in central London. At Paddington Station alone are 52 instruments installed which measure the 3D positions of more than 1800 prism targets several times per day (Leica Geosystems AG, 2014b, p 18 -21).

Similar systems are also set up in Rome for the monitoring of building movements due to the construction of the new underground line Linea C. Several total stations are placed at different locations in the city centre and permanently measure 3D displacements of historic sites like the Colosseum or the Forum Romanum. The data of these instruments is transmitted to a central processing station where the current coordinates of the monitoring points are calculated. Figure 2 shows the setup for monitoring the historic Trajan's column. A total station is installed on a surveying pillar and protected by a glass box from environmental impact. However, as it is shown in Lienhart (2017), measurements through glass windows can severely distort the results and thus in many monitoring installations the glass windows are omitted. The instrument automatically measures the current position of several prism targets mounted at different heights of the Trajan's column. In this setup vertical displacements (settlements) as well as tilt changes of the column can be determined. If threshold values are exceeded counter actions are initiated. In many cases, the counter actions include compensation grouting to bring the object back to its initial position. Such a procedure was successfully implemented during the extension of the Jubilee Line in London. The clock tower with Big Ben started tilting due to the nearby construction of a new underground station. Several compensation grouting campaigns were performed to keep the overall tilt change within the

predefined threshold limits. The whole procedure was monitored by total station measurements to prism targets mounted on the clock tower (Kavvadas, 2003).



Figure 2 Monitoring of the historic Trajan's column with a robotic total station and prism targets

4. LASER SCANNING

4.1 Principle of laser scanning

Laser scanners are able to perform reflectorless distance measurements at a very high frequency. In order to scan an object the emitted laser beam is sequentially steered into different directions. This can be realised by continuously rotating a mirror along a horizontal axis and turning the whole instrument along its vertical axis. The emitted laser beam is reflected by the object and part of the reflection is backscattered to the instrument. This signal is recorded and converted into a distance value. Together with the stored direction angles, a 3D point cloud in the local coordinate system of the laser scanner can be calculated. Modern laser scanners measure up to 1 million points per second and thus a full dome scan can be made within minutes. The point clouds of individual setup positions can be combined in a registration step into a global point cloud. Depending on the requirements of the application (short range and high precision, fast data acquisition, long range) different laser scanners are available. Table 2 lists specifications of different types of laser scanners. It can be seen that the distance precision varies between hundredths of a millimetre and several millimetres and that ranges can vary between less than 40 m and up to 2.5 km.

Table 2 Specifications of selected laser scanners (Surphaser, 2015; Leica Geosystems AG, 2017; Riegl, 2017)

Scanner	Speed	Range	Precision of distance
Surphaser IR_100HQ	1 million points per second	35 m	0.07mm @10m
Leica P50	1 million points per second	> 1km	3mm + 10 ppm
Riegl VZ2000i	500 000 points per second	2.5km	3mm

Laser scanning can be used to assess how the geometry of an object changes over time but also used to detect differences of the real geometry with respect to a design geometry. However, it is important to note that laser scanner measurements are mainly sensitive to deformations in the measurement direction. In plane deformations cannot be directly derived from laser scan data.

4.2 Pipeline assessment with laser scanning

In this application, laser scanning is used to evaluate the geometry of a water pipeline (Figure 3) which consists of more than 500 segments. Each segment has a length of 3 m and a diameter of 3.7 m and is constructed from a metal plate which was formed into a cylinder with both plate ends welded together. Due to this construction process the cross section geometry deviates from the ideal geometry of a circle. This is especially the case in the vicinity of the welding seam.

A high precision laser scanner was used to determine the size of the so called roof topping and to derive the misalignment at the location of the welding seam.



Figure 3 Water pipeline in steep terrain with more than 500 individual segments

Figure 4 shows the point cloud of one scan. Due to the high resolution and high precision of the laser scanner details like welding seams are clearly visible. The challenge of today's laser scanning is not the data acquisition but the automated analysis of the huge amount of data. Millions of collected points have to be condensed in an automated way to obtain the desired information.

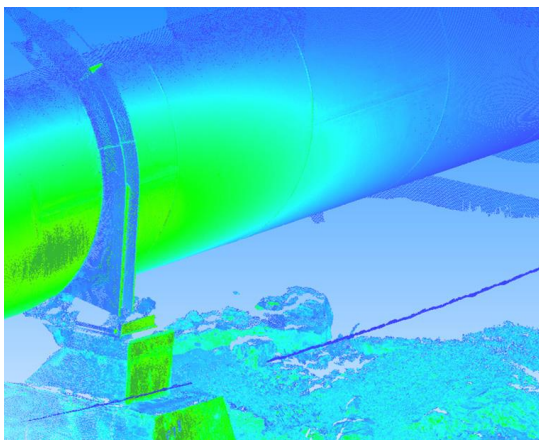


Figure 4 Point cloud of a scan of the water pipeline. Colors represent the intensity of the backscattered laser beam

In case of the pipeline, a cylinder is fit into the point cloud of every pipeline segment. In the next step profiles orthogonal to the axis of the cylinder are generated. Figure 5 shows to point distribution of one profile. All points left of point A and B are used to fit a circle into

the profile. Therefore, deviations in the vicinity of the welding seam do not affect the result of the circle fit. The area between points C and D covers the welding seam which can be clearly identified in Figure 5 right. Furthermore, it can be seen that about halfway between A and C and halfway between B and D the profile starts to deviate from the circle and instead of being on a curved line, the scanned points are on a straight line shown in white in Figure 5. It has to be noted that the size of the welding seam is less than 5 mm and it is remarkable with what detail the seam can be resolved with the high resolution laser scanner.

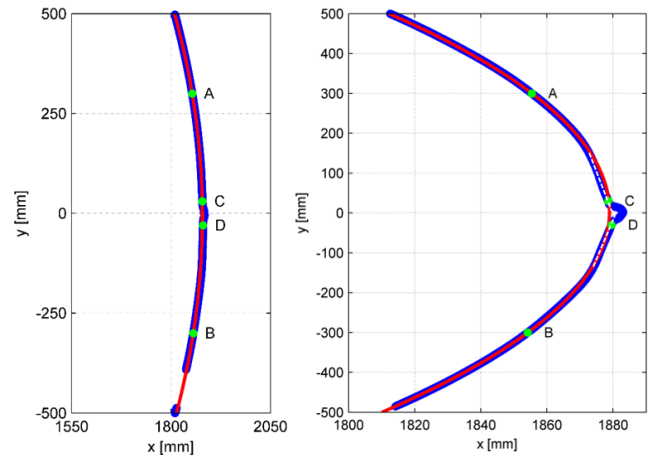


Figure 5 Point location (blue) of one cross section of the pipeline scan with fitted circle (red), left: same scaling of both axis, right: different scaling of axis to highlight details

4.3 Monitoring of retaining walls with kinematic laser scanning

About 10 years ago, laser scanning of large structures required the setup of the laser scanner on several static points. This was time consuming and often in conflict with the general use of the object.

Today, laser scanners can also be mounted on moveable platforms like planes, UAVs, trains or cars. This opens new possibilities. In many alpine areas retaining walls are monitored in regular intervals using conventional measurement techniques. These are for instance total station measurements to reflective targets on the retaining walls. Such measurements are time consuming and usually require the closure of highway lanes. Furthermore, the whole structure is only monitored on a few distinct points and large portions of the object remain unobserved. In order to obtain a complete picture of many retaining walls of a road network in an efficient way, mobile mapping systems (MMS) can be used. We apply this strategy and use the MMS shown in Figure 6 to assess the current state of the retaining walls of the Austrian highway network.

The measurement platform consist of a geodetic GNSS antenna and receiver, two laser scanners, an inertial measurement unit (IMU), an odometer and six cameras.

All sensors are calibrated to each other and the whole platform can be mounted on a regular car. We record data with driving speeds of up to 100 km/h and thus do not influence the traffic flow on the highway. Data of all sensors is collected continuously and the data analysis is performed in post-processing. First, the GNSS data is used together with reference station data of the Austrian positioning service (APOS) to determine the position of the platform.

Together with the IMU data, the position and orientation of the platform are known at any time. Combining this information with the data of both laser scanners yields georeferenced point clouds. An example is given in Figure 7. Due to the high measurement rate of the laser scanners, each scanner measures 1 million points per second, high resolution points clouds are obtained even at high driving speeds. The colours in Figure 7 indicate the intensity of the reflected light

beam. Green colours represent high intensity, blue colours low intensity. It can be seen that the retaining wall made of concrete reflects the signal well, whereas vegetation and asphalt return a weak signal.



Figure 6 Mobile mapping system mounted on a regular car passing by a typical retaining wall of the Austrian highway

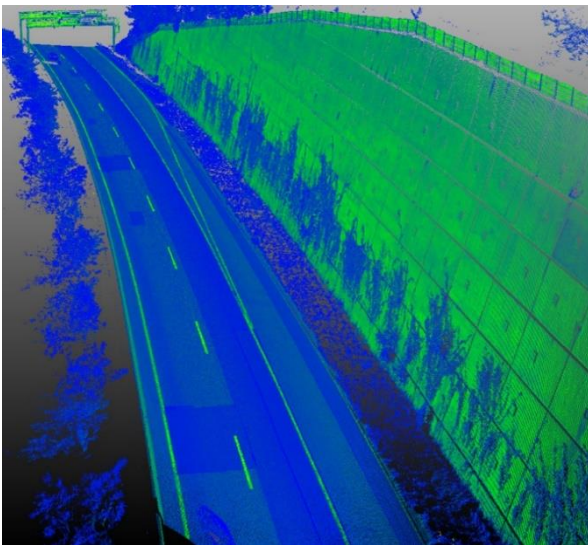


Figure 7 Georeferenced point cloud of a retaining wall

In the subsequent processing we automatically determine the tilt of the retaining walls and detect local deficiencies. More details of the processing can be found in Lienhart & Kalenjuk (2017). Depending on the roughness of the retaining walls, the tilt of the walls can be derived with a precision between 0.007° and 0.074° (Lienhart et al., 2017). Since the mobile platform scans the whole structure we are also able to identify local deficiencies. These are characterized by significant deviations from the general geometry of the retaining wall. In order to observe changes, the data collected at different times can be compared. It has to be noted that with respect to absolute position changes the accuracy is limited to the accuracy of GNSS phase fixed solutions. The accuracy of relative changes e.g. the determination of tilt changes can be performed with much higher accuracy. Tilt changes between individual measurement epochs can be determined,

depending on the size and structure of the retaining wall, with accuracy of better than 0.1° or 0.01° .

However, it is crucial to separate defects of the wall from measurement artefacts caused for instance by vegetation. Figure 8 shows a typical result. Significant deviations from local planes correspond to vegetation (a), horizontal joints (b) and anchor heads (c) but are also caused by to a local deficiency (d) where concrete has been fallen of. Besides geometry information we use the colour information from the images captured with the six cameras of the platform to aid the classification of the results. With this approach, concrete deficiencies can be separated from vegetation due to the different colour properties. Current research focuses on a unified procedure taking into account all available information of the point cloud, namely geometry information, RGB colour information and information about the reflectivity of the object.

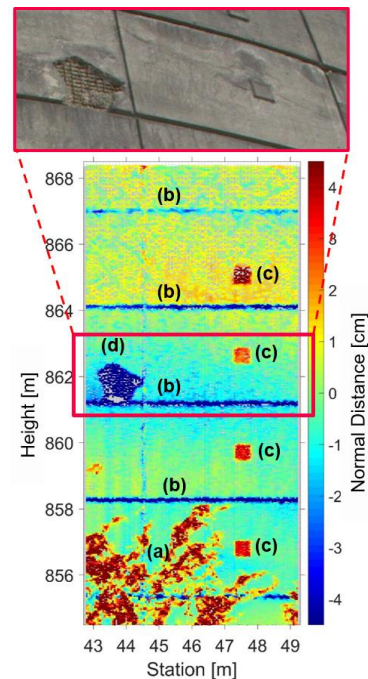


Figure 8 Difference values from local planes caused by vegetation (a), horizontal joints (b), anchor heads (c) and local deficiency (d)

5. IMAGE BASED MEASUREMENTS

5.1 Principle

As was shown in the previous example images can be used to aid the interpretation of monitoring data. However, still images or image sequences can also be used to derive deformation information. Very popular are currently UAV surveys where an object is captured from various different positions and angles by a camera mounted on the UAV. Usually 3D point clouds are calculated from the images using well known photogrammetric methods like bundle adjustment supported by ground control points with known coordinates. Many of these methods have significantly evolved with the massive increase of computer processing power. For the 3D reconstruction Structure from Motion (SfM) techniques are often used to generate in a first step sparse point clouds which are densified in a subsequent step. The point clouds derived from images can be analysed in similar ways as point clouds of laser scanners. Nevertheless, current laser scanners still deliver more accurate point clouds as camera images.

Images can also be beneficial in other ways. First, images are also able to identify structural deficiencies, which do not manifest themselves in geometric changes. Second, different to laser scanning, images are well suited to monitor movements orthogonal to the line of sight. Both aspects are exploited in more detail by the following examples.

5.2 Automated surface assessment of large water dams

The surface documentation of large water dams is conventionally carried out by the manual recording of damages with digital cameras. The captured images are assessed manually and identified damages are manually converted into CAD drawings. This process is labour-intensive, subjective and the detection of changes is difficult because images taken at different times are often taken from different locations. The surface documentation can also be carried out with automatically steered cameras. For this purpose we use the internal cameras of modern total stations. Latest versions of these instruments are equipped with an overview camera (OVC) and a telescopic camera (OAC, on axis camera). The OVC captures a larger area of the object of interest with a lower resolution, while the telescopic camera benefits from the 30-fold magnification of the telescope and can also detect details at a great distance (Figure 9).



Figure 9 Images of a water dam captured with the cameras integrated in a modern total station

Taking the field of view (FoV) into account, one pixel of the overview camera corresponds for instance to 10 mm at a distance of 100 m and one pixel of the telescope camera is 1 mm at a distance of 100 m (Leica Geosystems AG, 2015).

In addition to imaging, modern total stations are also capable of performing laser scans. Although the scanning speed is much slower than the scan speed of full laser scanners, the combination of scanning data and images with only one instrument can be beneficial. The major drawback of the conventional surface documentation of water dams is that no metric information like the size of the damages can be derived from the images. In Kalenjuck & Lienhart (2017), an approach is presented which overcomes this limitation.

The basic idea is that the water dam is scanned in the first measurement epoch. A surface model is derived from the registered and filtered laser scan data and can be used for the first and all subsequent documentation epochs. Subsequently, images from the surface are captured automatically with the motorized total station. Due to the small field of view of the telescopic camera, 1.5° with the used instrument, a documentation of the entire water dam with the OAC is too time consuming. Therefore, the locations of known damages are stored in a database and the instrument only aims to these areas in order to record high detailed OAC images. In addition to this, the entire water dam is captured with the overview camera. Due to the larger field of view, 19.4° with the used instrument, significantly less images are necessary. These images can be inspected for new damages. If new damages are detected in this coarse search, the OAC camera will also aim at these areas and record further high detailed images.

The captured images can be combined with the 3D model of the laser scan. One possibility is the texturing of the 3D model with the images of the total station. This is easy to realize, since the position and orientation of the camera are known and stored with each image. From the textured 3D model, 2D images can be derived again, but they now have metric information. In these images, a direct measurement of the size of damages is possible. The entire process is shown in Figure 10. It was applied to the Drossensperre, a large concrete arch dam located near Kaprun, Austria. This dam has a crown length of 357 m and a maximum height of 112 m. As described above, images of the entire dam were taken with the OVC and only selected areas captured with the OAC. These areas appear slightly darker in Figure 11. The enlargement of Figure 11 shows the generated ortho-photo of a sintering. Although this image looks very uniform, it consists of 21 individual images of the OAC. It can be used in further analysis to automatically determine the size of the sintering and its change with time as shown in Kalenjuck & Lienhart (2017).

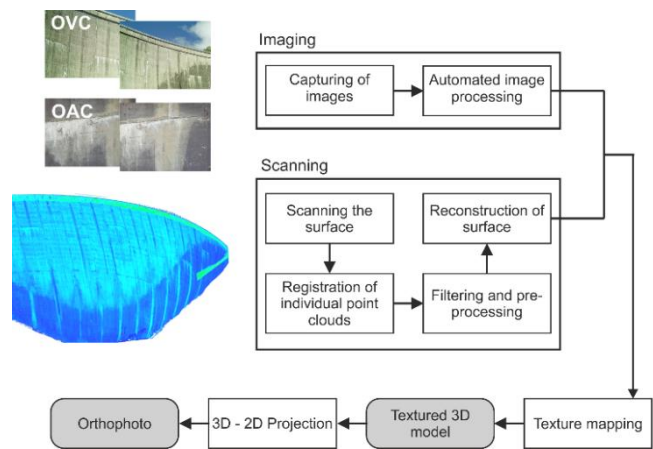


Figure 10 Combined analysis of image and laser scan data to generate ortho-photos

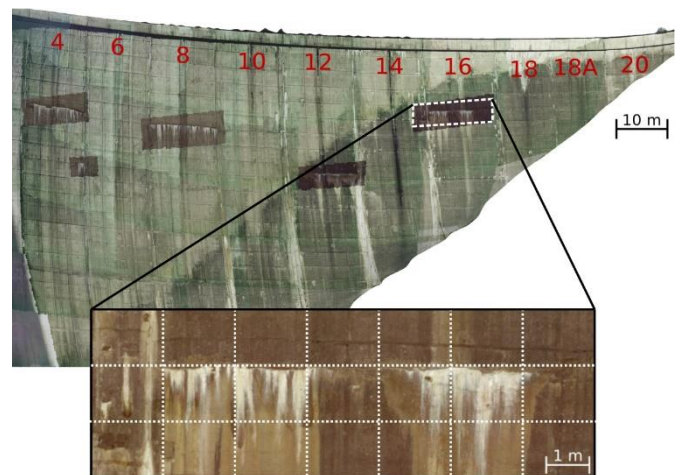


Figure 11 Textured surface model with OVC and OAC images

5.3 Monitoring of bridge vibrations using images

Modern cameras also enable the monitoring of fast moving structures. Therefore, video streams instead of static images are analysed. As it is shown in Ehrhart & Lienhart (2015) and Ehrhart et al. (2017) vibrations of foot bridges can be measured completely contactless using cameras.

Therefore, significant features of the object are identified and continuously tracked in the images. The big advantage compared to accelerometer measurements is that movements and their frequencies can be determined from the measurement data. Accelerometers are well suited to identify the frequencies of movements but the determination of movements is difficult because it requires double integration of accelerations whereby systematic errors like offsets or trends are magnified.

Figure 12 shows as an example the monitoring of vibrations of a footbridge. This bridge is 74 m long and video streams were captured from a distance of more than 30 m. The insert showing a bolt is a frame of the actual video used for monitoring. Different processing strategies like template matching, feature matching and optical flow were used to identify the position of the bolt in all images. The results of the image analysis in terms of frequencies and vertical movements were compared to independent reference measurements. Investigations reported by Ehrhart & Lienhart (2017) demonstrated that displacements can be determined with image assisted total station with better than 0.1 mm if all potential error sources are properly taken care of.



Figure 12 Footbridge and video frame of bolt used for monitoring

Figure 13 demonstrate that with all applied image analysis methods results similar to the results of the accelerometer measurements are gained. A more detailed analysis also for higher frequencies is given in Ehrhart & Lienhart (2015). Current commercially available image assisted total stations can record videos with a frame rate of 30 Hz. This is sufficient to identify Eigenfrequencies of large bridges, which are usually below 15 Hz. For higher frequencies clip on industrial cameras can also be used.

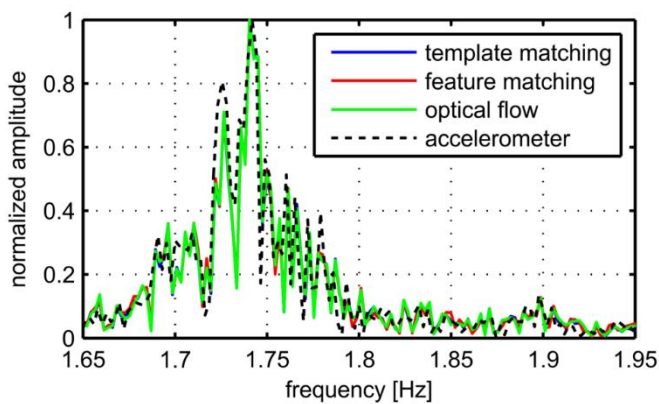


Figure 13 Frequency spectrum of bridge vibrations derived from image analysis and accelerometer measurements

Vertical displacements can also be derived from the image measurements. Therefore, changes with respect to the first frame are

calculated. The results were compared to reference measurements of a total station which tracked a prism mounted on the bridge. It can be seen in Figure 14 that the vertical movements were only in the range of a few tenths of a millimetre.

Interestingly, the results obtained with feature matching are in good correspondence to the total station measurements, whereas template matching and optical flow show a time dependent trend. A detailed investigation revealed that the increasing error is caused by accumulating snow (Figure 14 bottom).

This change of the image content resulted in a shift of the correlation peak of the template matching analysis. Feature matching proves to be more robust. The increasing snow height caused a reduction of the number of feature points but did not imply an increasing error in the calculated movement.

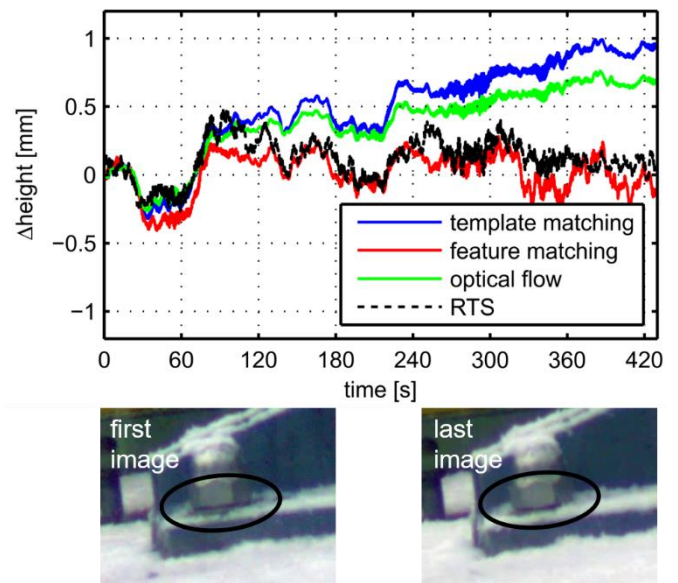


Figure 14 Vertical displacements derived with different image processing techniques and directly measured with a robotic total station (RTS) and prism (top), first and last image show increasing snow heights

6. GNSS MEASUREMENTS

6.1 Principle

Geodetic monitoring with Global Navigation Satellite Systems (GNSS) is based on phase measurements of the carrier wave of the signals transmitted by navigation satellites. These can be satellites of the US operated Global Positioning System (GPS), the Russian GLONASS, the European Galileo or the Chinese Beidou system. By using local reference stations or nationwide reference station networks real time positions can be determined with accuracies of 1 to 3 cm. In post-processing and using several hours of data accuracies can be improved to better than 1 cm.

Contrary to the other geodetic techniques discussed so far, the sensor, i.e. the GNSS antenna and receiver, has to be placed on the monitoring object. Therefore, a separate GNSS sensor is needed for every measurement point. Furthermore, power supply is also needed on all monitoring positions. This makes GNSS based monitoring expensive compared to other techniques, e.g. total station measurements where on total station can monitor a large number of relatively cheap passive prisms. However, GNSS based measurements offer unique advantages. One of them is the weather independence. Due to heavy rainfall, snowfall or fog other techniques like laser scanning, total station or image based measurement can fail, whereas GNSS measurements provide continuously 24/7 data even in such situations.

6.2 Landslide monitoring with GNSS

Their weather independence make GNSS sensors well suited for monitoring of landslides where large movements are often linked to heavy rainfall periods. We perform GNSS based monitoring of the landslide Gradenbach since 1999. Since then GNSS equipment as well as general communication technologies have evolved significantly. At the beginning of the monitoring in 1999, data was stored locally at the monitoring point, downloaded every few months and manually post-processed. Today, data is permanently streamed via the mobile phone network to a central server, where data processing runs automatically. Figure 15 displays the setup of the reference point on the mountain ridge. The GNSS receiver and modem are powered by car batteries which are charged using solar panels.

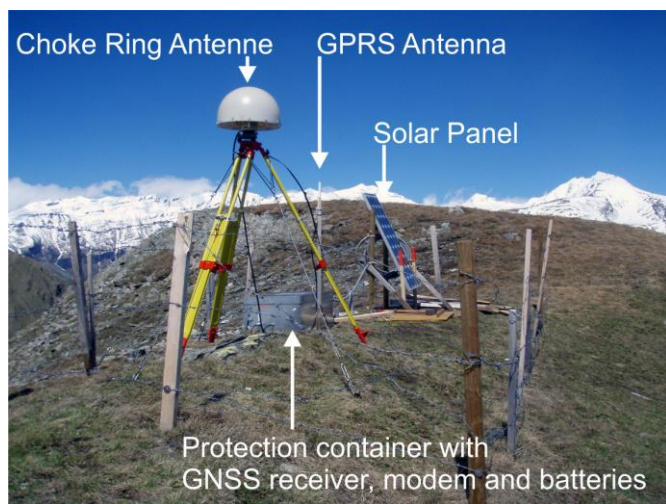


Figure 15 GNSS reference point R1 of the Gradenbach Observatory

In precise GNSS positioning reference points are used to eliminate influences of the atmosphere. The basic assumption of this differential positioning is that the atmosphere at the location of the reference point is almost identical to the atmosphere at the monitoring point. However, this is not the case if large height differences exist between reference and monitoring point.

Figure 16 shows the situation at the Gradenbach Observatory (Brückl et al., 2013). If only reference point Ref 1 is used the whole atmospheric impact between the height of monitoring point B and Ref 1 is not taken into account. This uncorrected atmospheric impact causes significant variations in the height component of point B and thus a high standard deviation (std). For the time window shown in Figure 16 middle, the std is 13 mm. Using a second reference station and applying our developed height correction model (Gassner et al., 2002) the standard deviation is reduced to 7 mm. It is astonishing that such high precision can be obtained with measurements to satellites which are orbiting more than 20 000 km above the earth's surface.

7. INTERFEROMETRIC RADAR MEASUREMENTS

Within recent years interferometric radar measurements became popular in geotechnical monitoring. Radar waves are sent out by a ground based instrument or by a satellite and the phase of the returning wave is recorded. Phase shifts can be derived from radar images taken at different times and these can be converted into distance changes in the line of sight of the instrument. If the instrument moves, e.g. due to the movement of the satellite or by moving the instrument along a rail (Figure 17) a synthetic aperture is generated which improves the cross range resolution.

The specifications of current ground based systems are given in Table 3. There are two important differences between laser scanning and radar measurements. Laser scanners measure absolute distances between the instrument and the target. Interferometric measurements

determine only the phase of the returning wave. If used for monitoring the deformations of the object must be small between measurement epochs. Secondly, the measurement spot of laser scanners is rather small, whereas radar measurements have a broader spatial resolution. For the ground based systems of Table 3 the spatial size of one measurement cell is in the range of several decimetres. The quality of the returning signal is strongly influenced by the reflection properties within each cell. If the object does not give enough reflection, corner cube reflectors made of metal or concrete have to be used. Common to both laser scanning and radar measurement is the sensitive axis in the line of sight. The big advantage of radar measurements is the very high distance resolution of 0.1 mm. With such a high resolution, movements can be detected already at an early stage, which is for instance important in case of rock falls to automatically close roads before catastrophic events happen.

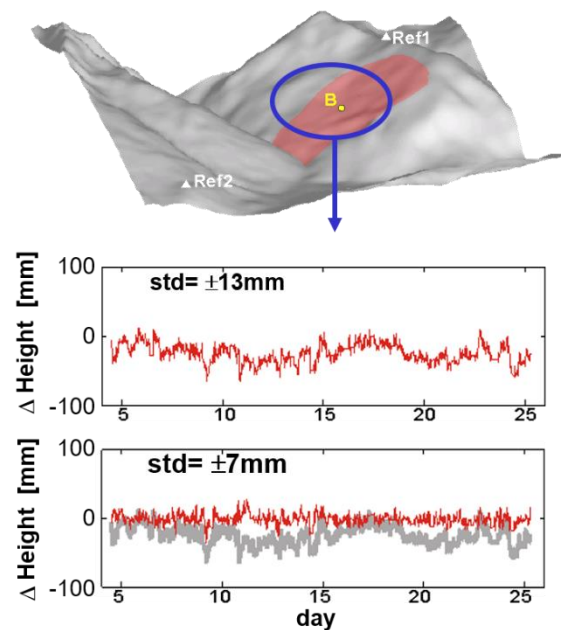


Figure 16 Height variations of monitoring point B at the Gradenbach observatory using one reference point (middle) and two reference points with height correction model (bottom)



Figure 17 Ground based synthetic aperture radar system moving along a rail

Table 3 Specifications of selected ground based synthetic aperture radar systems (IDS GeoRadar, 2017; Metasensing, 2017)

Instrument	Accuracy in line of sight	Spatial resolution	Range
IDS IBIS-FL	0.1mm	Range 0.5m Cross range: 4.4mrad	4.5km
Metasensing FastGBSAR-S	0.1mm	Range 0.5m Cross range: 4.8mrad	4.0km

8. CONCLUSION

In this article the current state-of-art of geodetic measurement techniques used in geotechnical monitoring was discussed. Modern geodetic techniques are capable to perform long-term measurements with millimetre or even sub millimetre accuracy over long distances and completely remotely. This is crucial especially in geotechnical monitoring where the structure, i.e. a rock face, may not be accessible due to safety reasons.

Today's geodetic instruments perform measurements fully automatically and thus can be used for early warning systems. Geodetic measurements are able to embed measurements of an object in an external reference frame and therefore not only determine relative deformations but also rigid body motions like settlements or tilt changes of a structure.

The potential of geodetic measurement techniques was demonstrated in this article with a range of examples from pipeline monitoring to landslide movements. Especially with kinematic data acquisition using mobile mapping systems, geodetic sensors truly digitize the real world and generate huge amount of data. With the current developments in big data analysis even more information will be gained from geodetic data in the near future.

9. REFERENCES

- Brunner, F. K., Rüeger, J.M. (1992) Theory of the local scale parameter method for EDM. *Bulletin Geodesique*, Vol. 66 S. 355-364, Springer Verlag
- Brückl, E., Brunner, F. K., Lang, E., Mertl, S., Müller, M., Stary, U. (2013) The Gradenbach Observatory—monitoring deep-seated gravitational slope deformation by geodetic, hydrological, and seismological methods. *Landslides*. June 2013, doi 10.1007/s10346-013-0417-1
- Ehrhart, M., Lienhart, W. (2015) Monitoring of civil engineering structures using a state-of-the-art image assisted total station, *Journal of Applied Geodesy* 9 (2015): 174 - 182
- Ehrhart, M., Lienhart, W. (2017) Accurate Measurements with Image-Assisted Total Stations and Their Prerequisites, *Journal of Surveying Engineering* 143(2): 04016024
- Ehrhart, M., Lienhart, W., Kalenjuk, S. (2017) Monitoring of bridge vibrations with image-assisted total stations. 4th Conference on Smart Monitoring, Assessment and Rehabilitation of civil Structures (SMAR), Zurich, Switzerland: 8 p
- Gassner, G., Wieser, A., Brunner, F. K. (2002) GPS software development for monitoring of landslides. In: *Proceedings of FIG XXII Congress*, Washington, D.C., USA. 12 p
- IDS GeoRadar (2017) IBIS-FL. Datasheet, 2 p
- Kalenjuk, S., Lienhart, W. (2017) Automated Surface Documentation of Large Water Dams Using Image and Scan Data of Modern Total Stations, *Proc. FIG Working Week 2017 Surveying the world of tomorrow - From digitalisation to augmented reality*, Helsinki, Finland: 15 p
- Kavvas, M. J. (2003) Monitoring and modelling ground deformations during tunneling. *Proc. 11th FIG Symposium on Deformation Measurements*, Santorini, Greece, 19 p
- Leica Geosystems AG (2014a) Leica Nova TM50. Datasheet, 2 p
- Leica Geosystems AG (2014b) Reporter - The Global Magazine of Leica Geosystems, Issue 71, 32 p
- Leica Geosystems AG (2015) Leica Nova MS60. Datasheet, 2 p
- Leica Geosystems AG (2017) Leica ScanStation P50. Datasheet, 2 p
- Lienhart, W. (2017) Geotechnical monitoring using total stations and laser scanners: critical aspects and solutions. *Journal of Civil Structural Health Monitoring*, 7(3): 315-324, doi 10.1007/s13349-017-0228-5
- Lienhart, W., Ehrhart, M. (2015) State of the Art of Geodetic Bridge Monitoring. *Proc. Int. Workshop on Structural Health Monitoring (IWSHM)*, Stanford, USA: 449 - 456
- Lienhart, W., Ehrhart, M., Grick, M. (2017) High Frequent Total Station Measurements for the Monitoring of Bridge Vibrations. *Journal of Applied Geodesy* 11 (1): 1 - 8
- Lienhart, W., Kalenjuk, S. (2017) Combined Laser Scanning and Image Based Monitoring of Large Infrastructure Objects. *Proc. Int. Workshop on Structural Health Monitoring (IWSHM)*, Stanford, USA: 3147-3154
- Lienhart, W., Kalenjuk, S., Ehrhart, C. (2017) Efficient and Large Scale Monitoring of Retaining Walls along Highways using a Mobile Mapping System. *Proc. 8th Int. Conf. on Structural Health Monitoring of Intelligent Infrastructure - SHMII-8*, Brisbane, Australia: RS3-11, 8 p
- Metasensing (2017) FASTGBSAR-S, Datasheet, 4 p
- Meyer, Ch., Eisensegger, St. (2011) *Durchmesserlinie Zürich: geotechnisches und geodätisches Monitoring für ein grosses innerstädtisches Infrastrukturprojekt*. *Géomatique Suisse* 4/2011: 140 - 145
- Michel, V., Person, T., Kasser, M. (2003) 74 Motorized Tacheometers Aiming at 5350 Prisms in Amsterdam: The Largest Topometric Continuous Real Time Monitoring System in the World? *Proc. FIG Working Week 2003, TS22 Surveying in Industry and Construction*, 9 p
- Riegl (2017) RIEGL VZ-2000i. Datasheet, 10 p
- Rüeger, J. (1996) *Electronic Distance Measurement*. Springer Verlag Berlin Heidelberg New York, 4th edition, 276 p
- Surphaser (2015) SURPHASER - 3D LASER SCANNERS. Datasheet, 2 p
- Topcon (2016) MS AXII Series. Datasheet 4 p
- Trimble (2017) Trimble S9/S9 HP. Datasheet, 4 p